CHAPTER 2

STUDY OF A UNIAXIAL TENSION TEST METHODOLOGY

2.1. INTRODUCTION

This chapter deals with the development of a uniaxial tension test methodology for steel fiber reinforced concrete. The importance of the study resides mainly in the fact that uniaxial tensile loading conditions are considered to be the most general failure mode for quasi-brittle materials like concrete, and that there is no consensus about a standard method to evaluate the behavior under such a loading state. The main objective of this chapter is to study a complete, robust and practically-viable procedure to carry out the uniaxial tension test.

Tests are carried out on circumferentially-notched molded cylinders and cores of different strength levels and volume fractions of fibers. Along with practical issues, the mode of failure and the stability of the test response will be of main interest, together with the variability of the results and their sensitivity to fiber content. Furthermore, since flexural tension is the most commonly used procedure to evaluate the toughness, three point bending tests are also carried out for possible comparisons between two responses.

2.2. REVIEW OF UNIAXIAL TENSION TESTING METHODS

For steel fiber reinforced concrete (SFRC), the most important aspect of its mechanical performance is probably the tensile behavior. However, as in all brittle matrix composites, a uniaxial tensile test is difficult to perform, especially if the post-peak response is desired. However, there are several studies where uniaxial tension tests have been performed. Some studies use relatively thin coupons (i.e., panels or bars of 20 mm thickness without notches) of FRC for obtaining the complete response (e.g., Li et al., 1998). The main problem in such tests is that the failure may occur at the grips (due to stress concentrations and multiaxial stresses). To avoid such failure, the ends of the specimen are often clamped to the grips through rubber pads (e.g., EFNARC standard, 1993). Another approach for avoiding this problem is the use of "dogbone" panels with a reduced central cross-section, where the cracking occurs, which also facilitates the measurement of displacements (Banthia et al., 1993). This configuration also provides for the stable control of the test as long as the failure is the cracking does not occur outside the gage length of the displacement sensors.

Realizing that the cracking behavior is of interest in FRCs, a number of test configurations have been proposed based on notched specimens (e.g., double-edge-notched panels), where a single crack is forced to occur along the notch plane, which can then easily be monitored. There are, however, two important issues that should be addressed in such tests: the stress concentration at the notch tips, that leads to a lower tensile strength, and the test control that needs the average of the two notch openings.

Panels with notched edges have been used to obtain the tensile response of FRCs, including the tensile stress versus crack opening relations (Gopalaratnam and Shah, 1987; Mobasher and Shah, 1989; Wecharatana, 1990; Aarre, 1992; Cho et al., 1992). When the complete load-displacement curve can be measured, the area under the curve can be divided by the net cross-section area and taken as the fracture energy, which is considered to be a fundamental measure of the toughness of the material.

For SFRCs with normal-size aggregates and isotropic fiber distributions, thin panels are not representative of the material and, therefore, tests have to be performed on larger specimens. For example, Wang et al. (1990) used a prism with a notch along the perimeter, which was glued to the steel loading plates. The use of notched cylinders is more appealing since molded cylinders are the standard specimens in most countries for determining the compressive strength. Moreover, the methodology can be also applied to cores extracted from structural elements. The specimen is usually instrumented with clip gauges or extensometers measuring the crack opening over the notch. The signal is averaged and provides a feed back signal for closed loop control.

There has been some debate on whether the results obtained are material properties free from structural effects. Hordijk (1991) carried out a detailed investigation of the influence of specimen size, geometry and the boundary conditions on the results of uniaxial fracture tests on plain concrete. He concluded that the uniaxial fracture test is the only test that yields directly all relevant fracture parameters even though care must be taken to minimize effects of structural behavior of the test specimen on the measured results. These structural effects can never be completely eliminated, however some guidelines are set up for design of deformation controlled uniaxial tensile tests.

Another issue that is controversial is about the end conditions in the test. Van Mier argues that the use of fixed boundary conditions (high rotational stiffness of the loading platens) promotes the formation of several crack planes resulting in an artificial increase in crack density (van Mier et al., 1996). Thus, the measured fracture toughness will be artificially increased. Nevertheless, the use of rotating ends increases the bending and non-symmetric displacements in the specimen, which is especially relevant for the post-cracking response of FRC. Cattaneo and Rosati (1999) experimentally studied the effect of the boundary conditions with interferometry. They observed a more even cracking in the critical cross section and a more uniform strain field, with fixed platens.

Notched cylinders have been used by several researchers in uniaxial tension tests: Stang and Bendixen (1998) used 130 mm diameter cylinders with a 10 mm deep notch, Groth and Noghabai (1996) tested cores of 70 mm of diameter and 170 mm in length with

a smooth semicircular notch of 10 mm radius, Plizzari et al. (2000) used 80 mm diameter and 210 mm high cylinders (notch depth = 4 mm), and Rossi (1997) used 74 mm diameter and 60 mm height specimens with a 15 mm deep notch.

The stress-crack width relationship is generally extracted from the experimental load and average displacement data. Stress is referred to the notched cross section, while the crack opening is taken as the measured post-cracking displacement (see e.g., Petersson, 1981; Hordijk et al., 1989).

Recently, a complete recommendation for the uniaxial tension testing of SFRC has been given by RILEM TC 162 TDF (2001). A notched cylinder of 150 mm diameter and 150 mm height is proposed. The specimen is glued to the loading plates and the test is controlled by the average of at least three displacements measured at equal distances along the perimeter of the specimen. This recommendation will be taken as the base for the uniaxial tension test studied in this chapter.

2.3. CHARACTERISTICS OF THE PROPOSED METHODOLOGY

2.3.1. Background

To design a viable test method, the following aspects should be considered:

- Requirements related to testing equipment
- Ease of execution
- Reliability of the test results

With relation to the first aspect, the following issues are important with respect to the testing equipment for the present type of test. The test setup, which includes the testing machine, the loading platens and junctions must be stiff enough to avoid the loss of stability after the first peak load. Misalignment of the specimen should be avoided to maintain uniaxial loading across the crack plane. When fixed boundary conditions are prescribed, end rotations should be reduced with stiff fixtures. Displacement-controlled

tests require closed-loop servohydraulic testing systems, with transducers appropriately mounted to provide the feedback signal needed for the control variable.

In terms of the execution, it is desirable that the specimen dimensions correspond to commonly-used moulds, the size and shape make it easy to handle, the test duration is within a practical range (say, 10-60 minutes) and does not require highly-trained technicians.

Obviously, the reliability of the results is of foremost importance. In the present test, it should be expected that the results are repeatable (considering inter- and intra-laboratory comparisons), have a low scatter and are sensitive to the characteristics of the material tested.

2.3.2. Proposed Experimental Configuration

An Instron 8505 servo-hydraulic testing system with a 2000 kN static load carrying capacity, with a stiff frame, is used for the study (Figure 2.1).

Figure 2.1. Testing machine used in the study

The specimen was directly glued, in situ, to the loading platens of the machine. By eliminating soft connections between the specimen and the machine, the set up takes full advantage of the high rotational stiffness. Moreover, the in situ curing of the adhesive also minimizes misalignment and non-uniform loading.

The test is controlled by means of the average signal of three Epsilon extensometers of 2.5mm span and 25mm gauge length placed at 120º between each other, around the specimen (Figure 2.2). The sensitiveness of the feedback signal allows the use of loading rates in the order of 0.1 μm/sec. The feedback control is performed through the digital controller of the testing system (INSTRON 8500 Plus). The following loading sequence is used: an average crack opening rate of 5μm/min up to 50μm, then 100 μm/min from 50 to 1000μm and 500μm/min then onwards until at least 2000μm of crack opening.

For obtaining individual readings of the crack opening around the notch mouth, three LVDTs (of 5 mm span) were placed around the specimen at 120º in between the extensometers (see Figure 2.2). All readings are recorded electronically through the data acquisition unit of the testing system.

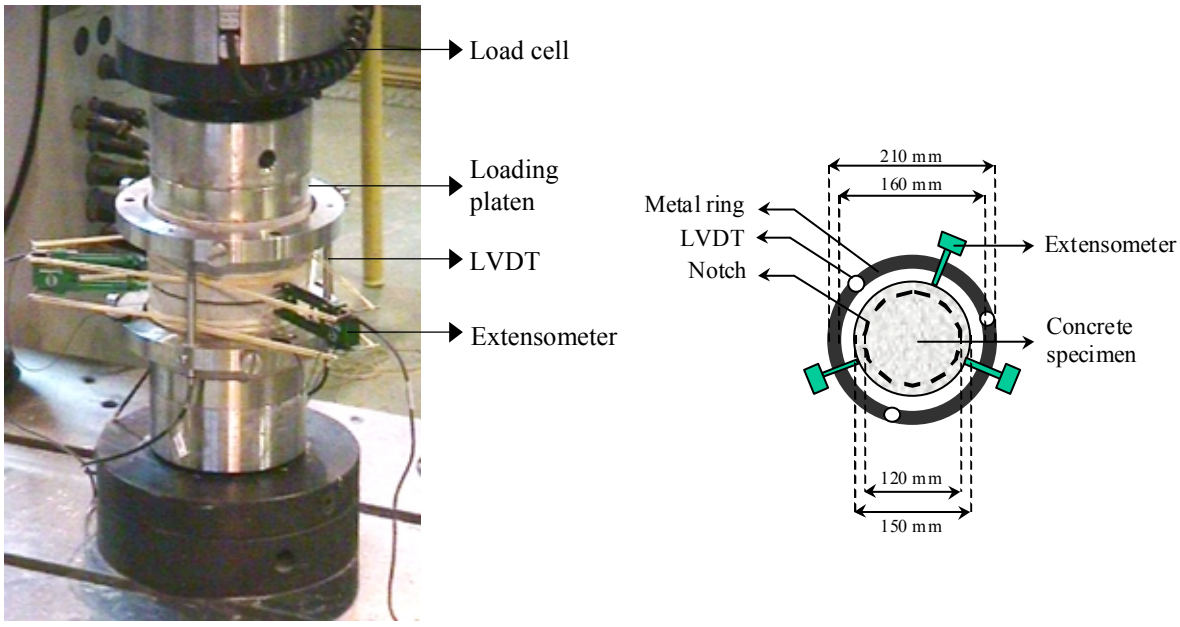

Figure 2.2. Test set-up

2.3.3. Specimen Preparation and Setup

The proposed uniaxial tension specimen of 150 mm diameter and 150 mm height is obtained from a standard 150×300 mm cylinder after cutting off a 75 mm thick slice from each end. A 10 mm deep circumferential notch is then cut at mid-height using a diamond-impregnated disc.

The surfaces that have to be glued to the loading platens are polished and then carefully cleaned with a solvent. If the cut is even, polishing is not essential since a the roughness of the cut surface could be beneficial for better adherence. After preparing the loading surfaces and cutting the notches, the specimen is fixed to the platens of the testing machine using a fast setting two-component glue (X60-NP Schnellklebstoff, HBM Wägetechnik GmbH, Germany). The following gluing procedure is employed: first, the bottom of the specimen is glued to the lower loading platen of the testing machine and a small load applied (aprox. 0.5 kN) and kept for a few minutes. Then the upper face of the specimen is glued to the upper platen and again a small load is applied for approximately 15 minutes. It is important to note that the loading surfaces must be perfectly parallel to each other and perpendicular to the longitudinal axis of the specimen. Besides the already mentioned consequences of misalignment, an uneven distribution of glue thickness could cause non-uniform residual stresses due to the shrinkage of the glue.

Figure 2.2 shows the general test set up. The extensometers are mounted on the specimen through three-contact-point knife edges (see Figures 2.3 and 2.4). The LVDTs are mounted across two metal rings separated by 100 mm, which are fixed to the specimen with screws (Figure 2.2).

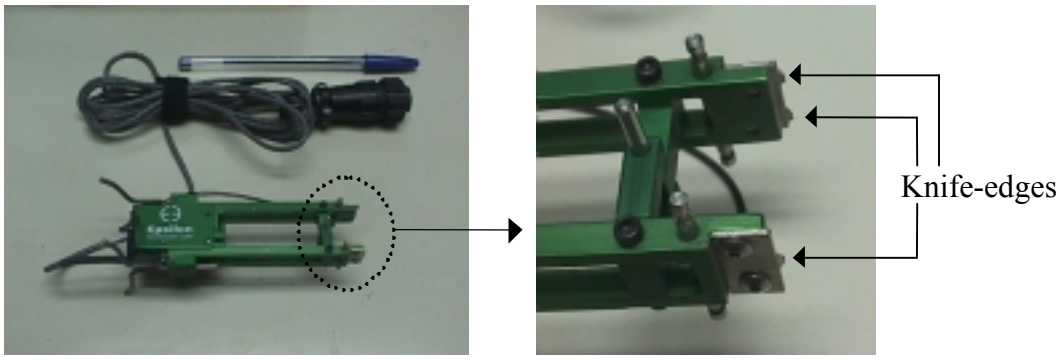

Figure 2.3. Extensometer

Figure 2.4. Mounted extensometer

2.4. EVALUATION OF THE TEST METHODOLOGY

The above methodology is evaluated in this section with tests of plain and steel fiber reinforced concretes using specimens that were fabricated within a European project at different laboratories. Normal and high strength concretes, with characteristic strengths of 25 and 70 MPa, respectively, were tested. The fiber dosages used in the two concretes are given in Table 2.1.

Table 2.1. Concretes tested

	Normal strength	**High strength**
Fiber type	Dramix® 65/60 BN	Dramix® 80/60 BP
Fiber dosage	0, 25, 75 kg/m^3	0, 25 kg/m^3

2.4.1. Failure Modes

In the tests of the normal strength concretes, the cracking generally occurred along the notch plane (Figure 2.5). However, in some cases, there was significant cracking outside the notch, as seen in Figure 2.6. The deviation of the crack from the notch plane was most common in the concrete with 75 kg/m^3 (Figure 2.7). This type of failure is undesirable since there is a loss of control in the test and sudden failure occurs. Also, the crack area cannot be estimated reasonably and, therefore, useful results cannot be obtained from the test. Such irregular failure implies that the notch depth of 10 mm maybe insufficient in this test for restricting the crack to the notch plane.

Figure 2.5. Typical failure

Figure 2.6. Failure outside the notch plane

Another problem in the tests is the possible failure of specimen at one of the ends, as in Figure 2.8. Again it appears that the notch depth used does not create a stress concentration at the notch tip that is large enough to avoid the failure at the ends.

Figure 2.7. Crack deviation outside the notch

Figure 2.8. Failure at the end

In the high strength concrete, no anomalous failure was observed, probably due to the higher brittleness of this concrete and to the low fiber content.

2.4.2. Stress-displacement Response

As mentioned earlier, the average crack opening displacement ($\bar{\delta}$) was obtained in each test using three extensometers, and individual crack openings (δ_i, i = 1,2,3) were measured at three different locations using LVDTs. Typical load (P) versus δ_i diagrams are shown in Figure 2.9. It can be seen that the individual LVDT responses may vary significantly for small displacements (see inset) basically due to crack propagation in the matrix but the fibre-dominated responses (i.e., beyond δ_i of about 100 μm) are quite similar in the 3 cases.

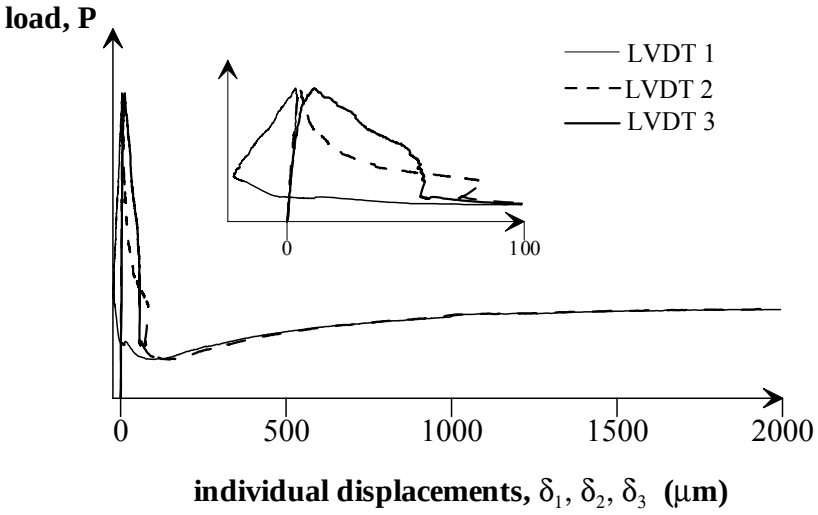

Figure 2.9. Typical responses of load versus δ_i obtained from 3 LVDTs

The mean displacements obtained directly from the average signal of 3 extensometers ($\overline{\delta}$) is compared with that obtained from the individual measurements δ_i Figure 2.10. It is clear that the mean response obtained from two measuring systems (extensometers and LVDTs) is practically identical. Therefore, when the individual readings are not needed, the directly obtained average is sufficient for the present test configuration. Accordingly, only the average reading of the three extensometers will be discussed hereafter.

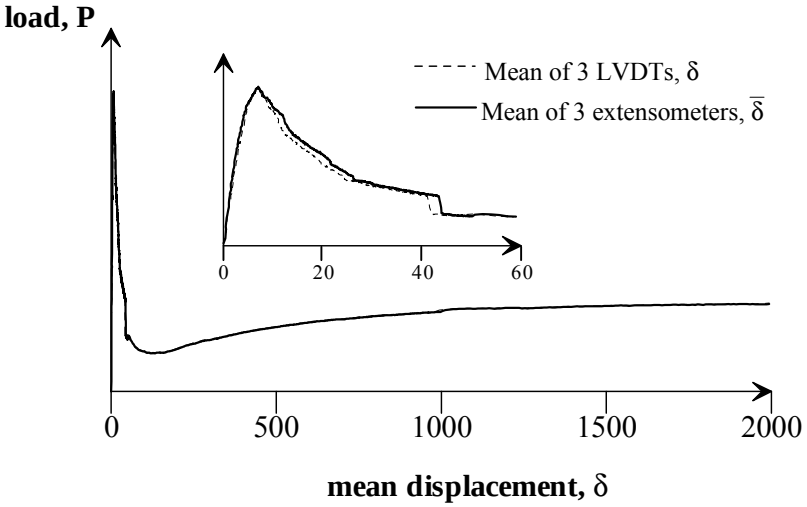

Figure 2.10. Load versus mean crack opening response

The load divided by the net area (or the area of the unnotched ligament) is considered as the applied tensile stress, σ (= P/A_{net}, where A_{net} = area of the ligament). The stress-displacement response can be used to obtain parameters that represent the material behavior. In the preliminary analysis performed in this chapter, the following parameters are considered for the analyses of the specimen response:

σ_{peak} = stress corresponding to the first peak

δ_{peak} = mean displacement at σ_{peak}

σ_{2000} = stress at 2000 μm of crack opening

The σ-$\bar{\delta}$ responses for normal strength concretes are given in Figures 2.11 to 2.13, and for high strength concretes in Figures 2.14 and 2.15. A closer view of the initial part of the response is shown in the plot on the right, in each case. Specimens in which the crack deviated outside the notch were not considered in the plots and the following analyses.

In all cases, the σ-$\bar{\delta}$ response is linear almost up to the peak with some non-linearity just before the peak load. In general, the responses exhibit very low scatter in the ascending branch (except for the case of plain NSC, where some scatter can be observed). An average variability of 15% has been observed in the first peak load (see Table 2.2). Once the peak load is reached, the load smoothly decreases with increasing deformation. In most of the cases, a sudden drop in stress is observed at the initial part of the post-peak response (as clearly seen in Figure 2.11), generally at a crack opening between 50 and 100μm. This is probably due to the crack propagation in the matrix, extending from one or more points on the notch tip perimeter. Probably, when the crack fronts coalesce, the drop in the σ-$\bar{\delta}$ response occurs.

On the other hand, after the peak, the SFRC specimens reach a minimum post-peak stress, beyond which there is either a plateau, as in Figure 2.12, or hardening-plastic response, as in Figure 2.13 or 2.15. Significant post-peak hardening is observed in some of the specimens with 75 kg/m^3 of steel fibers. In general, the variability increases in the initial part of the post-peak (say up to 35μm) and then remains practically constant until

the end of the test. On the other hand, the scatter observed at the beginning of the post-peak is comparable in plain and fiber concretes.

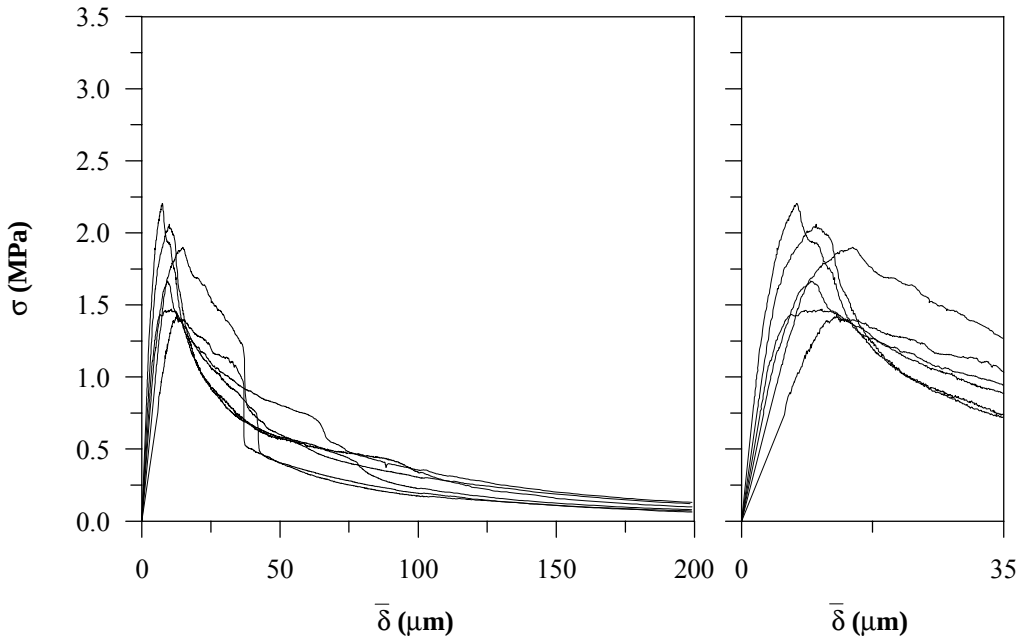

Figure 2.11. σ-$\bar{\delta}$ behavior for plain NSC

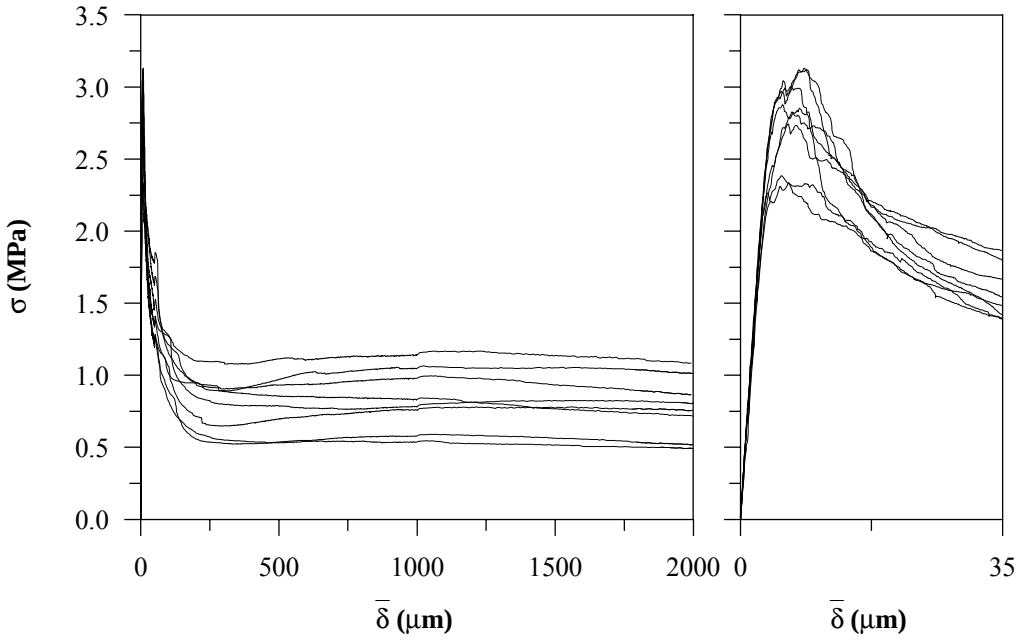

Figure 2.12. σ-$\bar{\delta}$ behavior for NSC with 25 kg/m^3

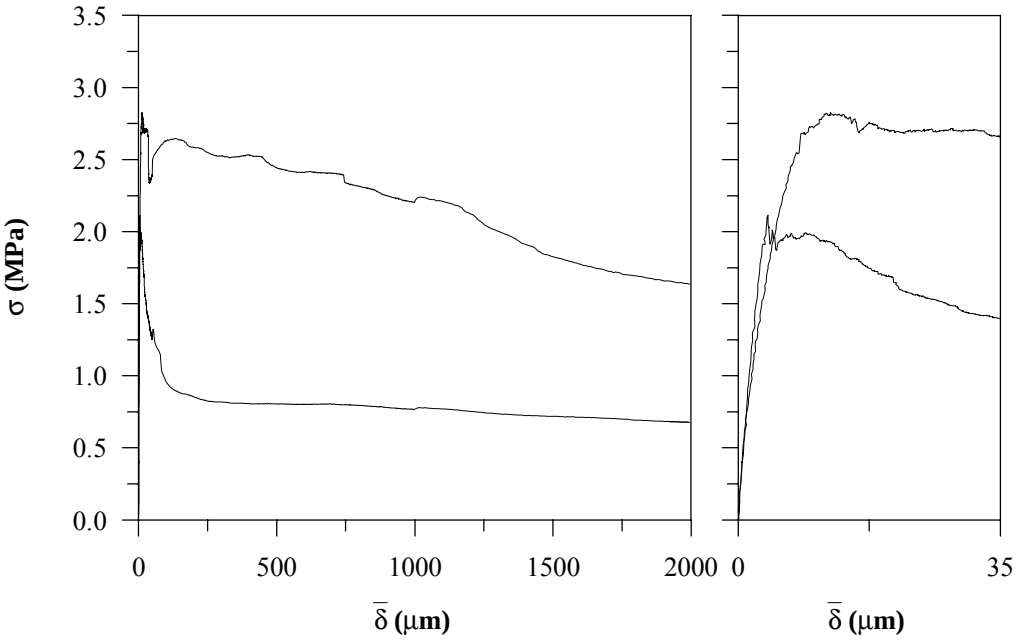

Figure 2.13. σ-$\overline{\delta}$ behavior for NSC with 75 kg/m^3

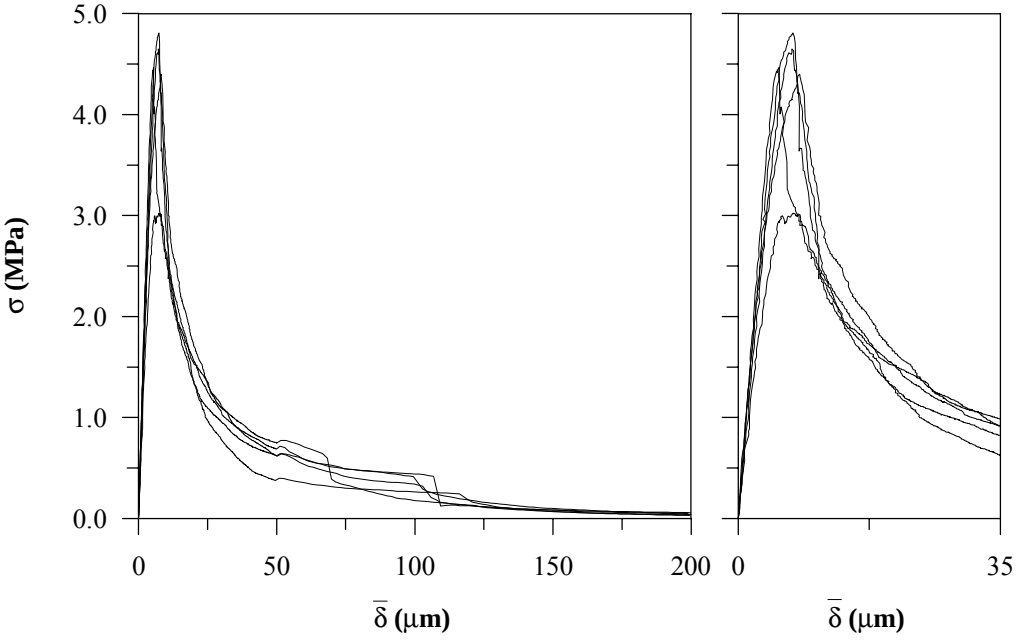

Figure 2.14. σ-$\overline{\delta}$ behavior for plain HSC

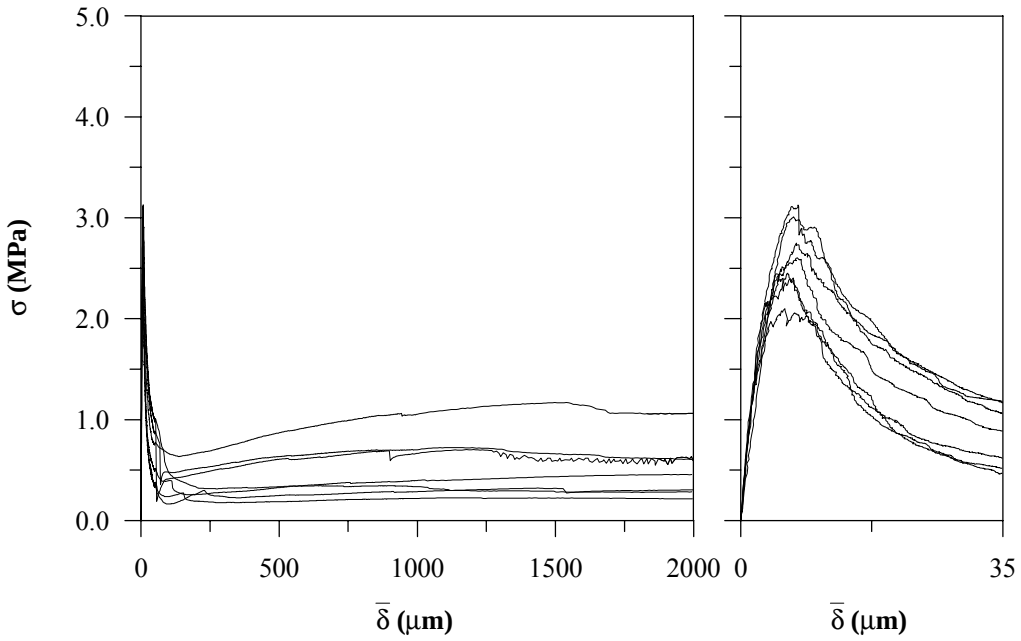

Figure 2.15. σ-$\bar{\delta}$ behavior for HSC with 25 kg/m^3

Table 2.2 presents the corresponding values of σ_{peak}, δ_{peak} and σ_{2000}, as mean values and coefficients of variation (COV). Neither the first peak stress, σ_{peak}, nor its variability seem to be significantly affected by fiber incorporation, as expected. Similarly, there are no significant changes in the peak displacement, δ_{peak}. However, the stress at the crack opening of 2000μm, σ_{2000}, depends on the fiber content; for example, there is an increase of about 50% when the fiber dosage increases from 25 to 75 kg/m^3.

Table 2.2. Peak and post-peak parameters

Concrete	**Fiber dosage**	**σ_{peak}** (MPa)	**δ_{peak}** (μm)	**σ_{2000}** (MPa)
C 25/30	Plain	1.79 (± 18%)	10.8 (± 24%)	—
	25 kg/m^3	2.81 (± 11%)	7.0 (± 18%)	0.78 (± 27%)
	75 kg/m^3	2.47 (± -%)	8.15 (± -%)	1.16 (± -%)
C 70/80	Plain	4.27 (± 17%)	7.1 (± 14%)	—
	25 kg/m^3	3.01 (± 13%)	7.1 (± 9%)	0.51 (± 53%)

2.5. APPLICATION TO CORES

Considering the possibility of applying the uniaxial tension test method for the evaluation of the material in existing structures, the behavior of cores has also been studied. With this aim, samples were extracted from halves of notched beams previously subjected to three point bending (see Figure 2.6). The corresponding flexural test results are presented in Annex A.

2.5.1. Materials

Two base concrete mixes have been studied, a normal strength concrete, with a characteristic compressive strength (f_c) of about 35 MPa, denominated C35 (mix N1) and a high strength concrete, designed to achieve an f_c of about 70 MPa, denominated C70 (mix N2). Table 2.3 shows the composition of the mixes.

In each mix, two dosages of steel fibers have been incorporated, 20 and 40 kg/m^3. In both cases, the fibers were non-coated, collated and hooked-ended, with circular cross section. The characteristics of the fibers can be seen in Table 2.4, where the quality of the steel is also indicated; in the case of N1, a low carbon steel fiber was incorporated and in N2, a high carbon fiber was used since they have higher strength.

Table 2.3. Mix proportions

Components	**Mix N1**			**Mix N2**		
	35/00	**35/20**	**35/40**	**70/00**	**70/20**	**70/40**
Cement ASTM type I (kg/m^3)	349			480		
Gravel 5-12 mm (kg/m^3)	978			921		
Sand 0-5 mm (kg/m^3)	873			840		
Silica Fume (kg/m^3)	-			48		
Water / Cement ratio	0.57			0.35		
Total water added (kg/m^3)	205			161		
Active naphthalene based superplasticizer (% of cem.cont.)	0.25			2		
RC-80/60 BN fibers (kg/m^3)	-	20	40	-	-	-
RC-80/30 BP fibers (kg/m^3)	-	-	-	-	20	40

Table 2.4. Characteristics of the fibers

Properties	**Dramix® fibre designation**	
	RC-80/60 BN (low carbon steel)	**RC-80-30 BP** (high carbon steel)
Aspect ratio	80	79
Length (mm)	60	30
Diameter (mm)	0.75	0.38
Minimum tensile strength (N/mm^2)	1100	2300
Modulus of elasticity (GPa)	200	200

2.5.2. Manufacturing of Specimens

In this study all mixes were elaborated using a 0.25 m^3 horizontal forced action mixer. The mixing procedure was as follows: first the coarse aggregate, then fine aggregate and the cement were loaded with the silica fume (in the case of high strength concrete). These components were mixed for 1 minute and after it the water was added and the mix continued for another minute, after it, the superplasticizer was incorporated. At this point,

for the case of plain concrete, the mixing continued for another 3 minutes and the process finished. For the FRCs, after pouring the chemical admixture, the mix continued for 2 minutes and then the fibers were incorporated and the components were mixed for another 3 minutes. No balling of fibers was observed and a satisfactory homogeneity was achieved. The mix presented an adequate workability. Slump test results of then fresh concretes are presented in Table 2.5, together with the standard properties.

Table 2.5. Characteristics of the concrete

Concrete	**Slump** (cm)	f_c (MPa)	E (GPa)
35/00	15	40.2	30.0
35/20	14	38.9	31.8
35/40	11	38.3	31.8
70/00	20	77.7	36.6
70/20	13	76.5	37.2
70/40	5	77.8	38.9

For each concrete, 150×300 mm cylinders and 150×150×600 mm beams were cast, from one batch. The specimens were table vibrated, using a 50 Hz vibrating table. The filling of the prismatic moulds followed the recommendations of Saldivar (1999) and RILEM TC 162 (2000a). After filling the moulds, the top surfaces were finished manually and covered with a plastic sheet. After 24 hours the specimens were taken out of the moulds and placed in a humid chamber (20 ± 2° C and 98% RH) during 28 days and then stored in the laboratory environment until the time of testing. The cylinder specimens were used to obtain the 28 day compressive strength (f_c) and the modulus of elasticity (E) given in Table 2.5.

2.5.3. Experimental Details

From the 150×150×600 mm beams, firstly a 25 mm long notch was cut with a diamond band saw at mid-length and perpendicular to the casting direction. Then the beam

was tested under three-point loading (3PL), with a 450 mm span. Deflections (δ) at mid-span and the Crack Mouth Opening Displacement (CMOD) were recorded. The test was controlled at a constant CMOD rate in a servo-hydraulic INSTRON system. The test details and results are presented in Annex A.

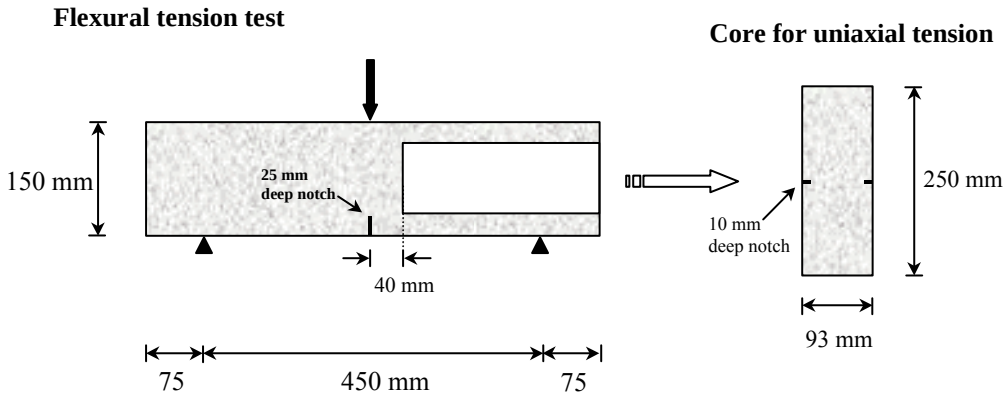

Figure 2.16. Obtention of Cores

After the flexure test, a 93 mm diameter and 250 mm long core was extracted from one of the halves of the beams, along the longitudinal axis (see Figure 2.16). Afterwards, an annular notch of 10 mm depth was cut at mid-height. Three cores were extracted and tested for each concrete mix. The notation used in the study is presented in Table 2.6 and is in accordance with the following designation:

N1, N2= Mix notations; the mix N1 corresponds to normal strength concrete (NSC) and N2 corresponds to high strength concrete (HSC)

UTC-p= Uniaxial tension test on a plain concrete cored cylinder of 93 mm diameter and 250 mm height.

UTC-20= Uniaxial tension test on a SFRC concrete cored cylinder of 93 mm diameter and 250 mm height containing 20 kg/m^3 of steel fibers.

UTC-40= Uniaxial tension test on a SFRC concrete cored cylinder of 93 mm diameter and 250 mm height containing 40 kg/m^3 of steel fibers.

The last number in the specimen notation denotes the trial.

Table 2.6. Specimen notation for uniaxial tension on cores

Test series	Fiber dosage (kg/m^3)	Specimen notation	
N1 (NSC)	0	N1-UTC-p	1~3
	20	N1-UTC-20	1~3
	40	N1-UTC-40	1~3
N2 (HSC)	0	N2-UTC-p	1~3
	20	N2-UTC-20	1~3
	40	N2-UTC-40	1~3

The test was carried out identically as for the case of molded cylinders (see Section 3), with fixed loading platens and under average crack opening displacement control, using the measurements of extensometers arranged across the notch at 120º from each other (Figure 2.17).

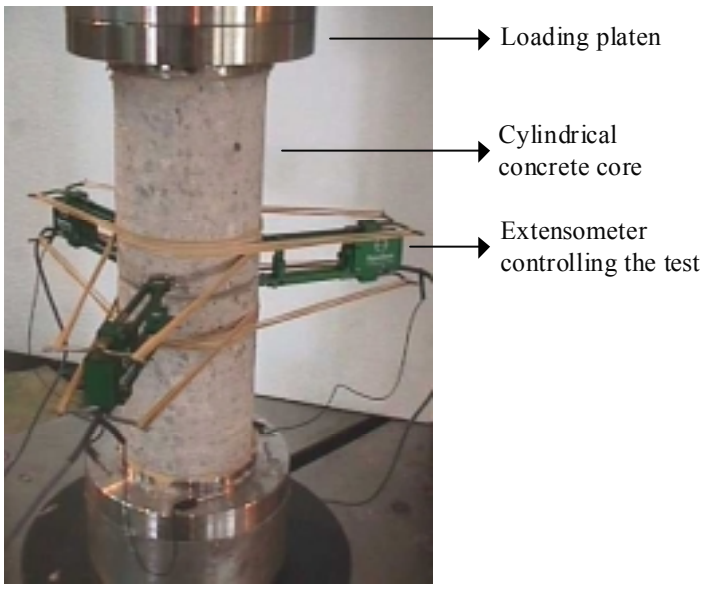

Figure 2.17. Configuration of the uniaxial tension test on cores

2.5.4. Test Results

In total, 18 cores were tested under uniaxial tension. All specimens failed through the notch planes and the tests were stable over the entire pre- and post-peak response. A typical fracture surface of a high strength SFRC specimen is shown in Figure 2.18.

Figure 2.18. Core fracture surface

The following sections will present the stress (σ) versus mean crack opening displacement ($\bar{\delta}$) response for all tested specimens. Both σ and $\bar{\delta}$ are calculated as previously explained in section 2.4.2.

2.5.4.1. Results of Tests on Normal Strength Concrete Cores

Figures 2.19-2.21 show the stress- crack opening displacement response of the NSC specimens tested. A zoom of the initial part of the response is presented at the right of each figure. The observed stress-crack opening response is similar to that of a molded cylinder, with almost linear pre-peak behavior and a smooth drop after the peak in the case of plain concrete specimens. For SFRCs the response reaches a minimum post-peak stress level after which either a plateau or a hardening stage is observed. Also, as in the case of molded cylinders, a stress drop appears in the σ-$\bar{\delta}$ response of some of the specimens at around a

crack opening of 30 μm. Other fact that can be observed in all the cases is the variability of the post-peak response. Visual observations confirm that the residual stresses are in accordance with the number of fibers on the failure plane; with more fibers for higher residual stresses. As an example, specimen N1-UTC-20-3 that shows almost zero residual stress (Figure 2.20) had only 1 fiber on the failure plane.

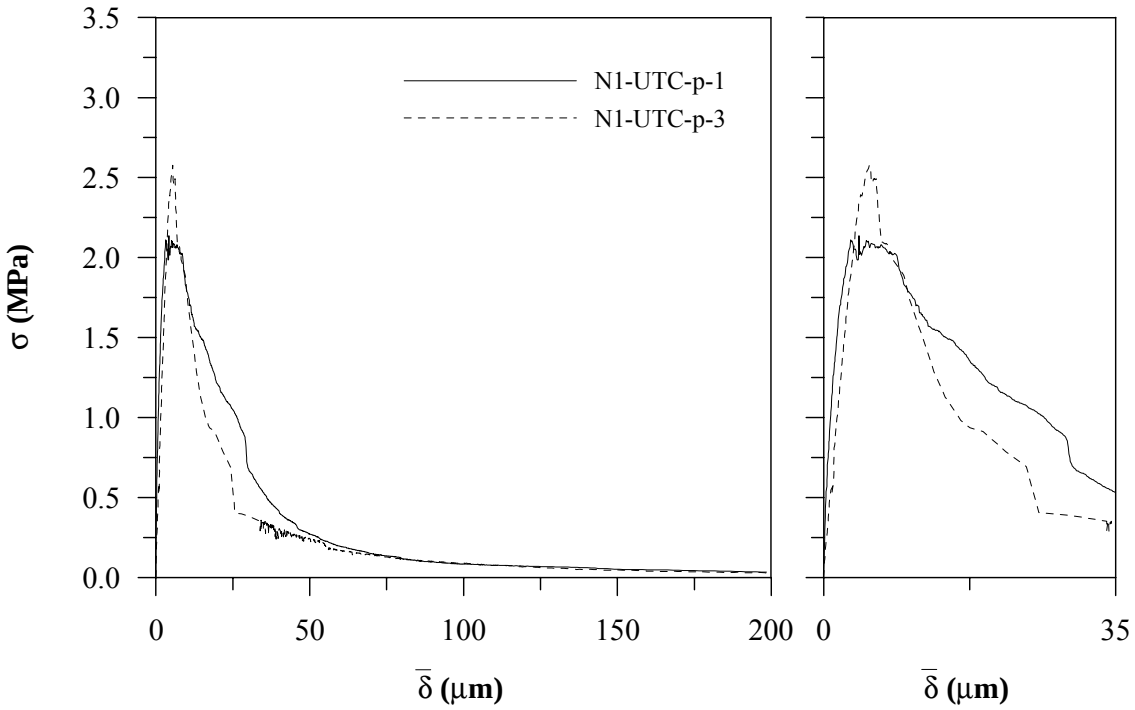

Figure 2.19. σ-$\bar{\delta}$ response for plain NSC cores

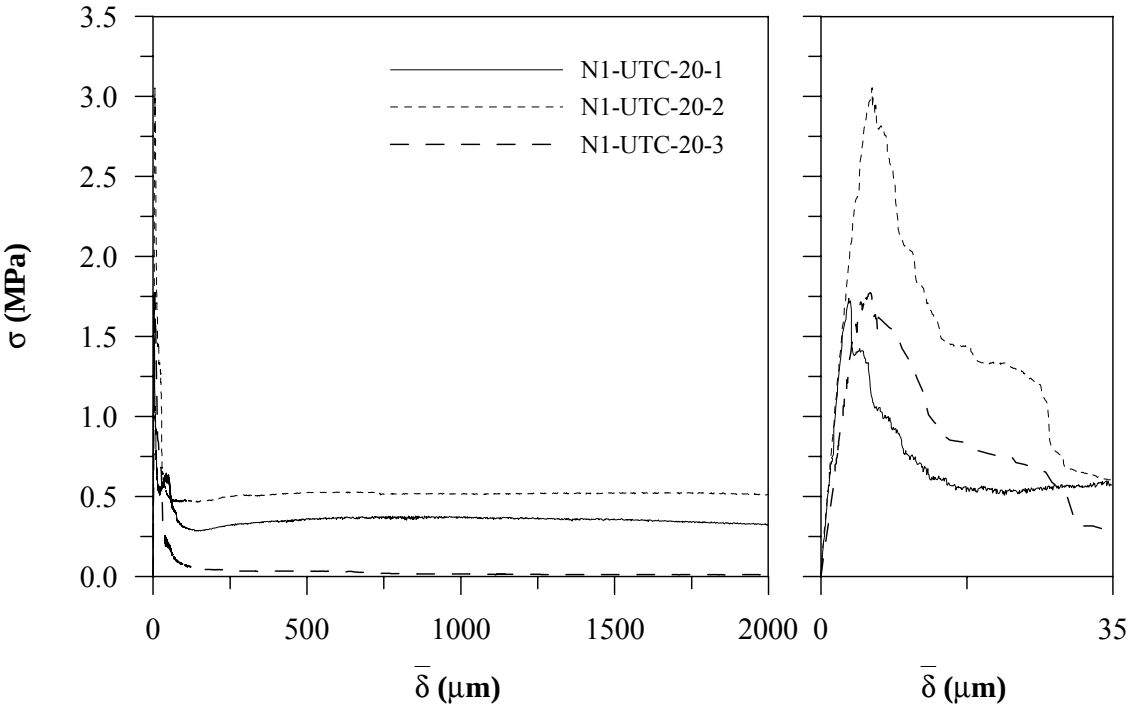

Figure 2.20. σ-$\bar{\delta}$ response for normal strength SFRC cores, 20 kg/m^3 of fibers.

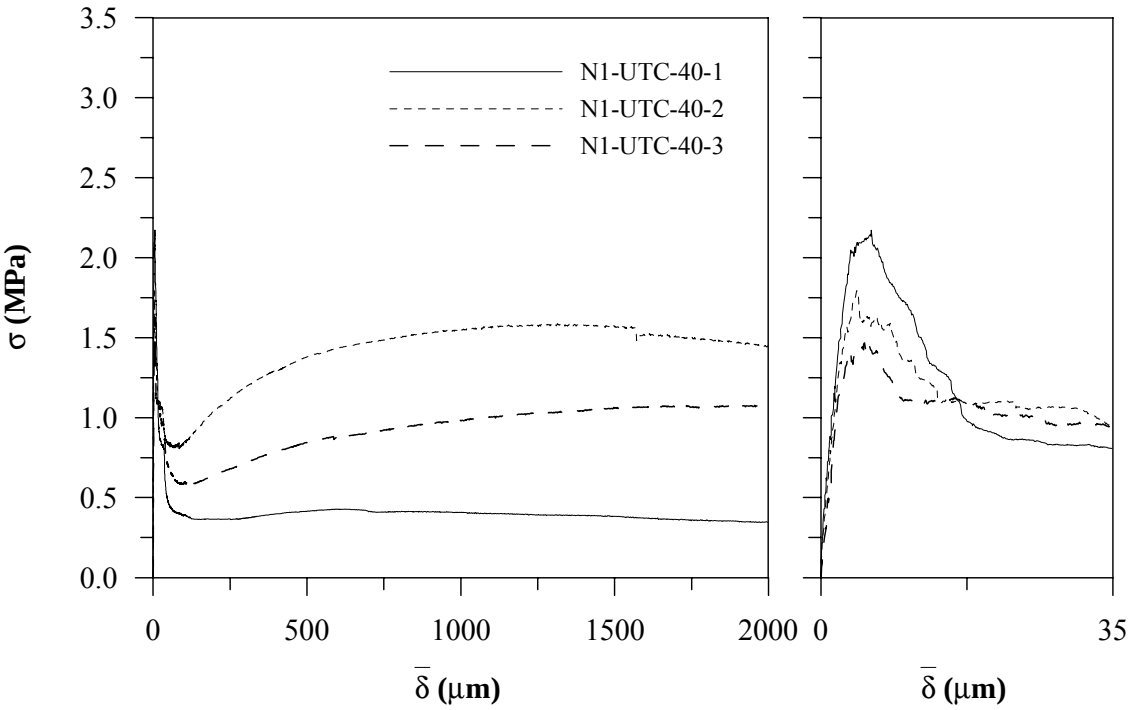

Figure 2.21. σ-$\bar{\delta}$ response for normal strength SFRC cores, 40 kg/m^3 of fibers.

Table 2.7 presents the average peak and post-peak parameters for the tested specimens, together with the coefficients of variation (COV) in parentheses. A slight decrease in σ_{peak} with fiber dosage is observed, probably due to lower compaction of the fiber concretes. On the other hand, the post-peak parameters (σ_{1000} and σ_{2000}) clearly reflect the fiber content. However, the variability of the parameters appears to decrease as the fiber dosage increases.

Table 2.7. Peak and post-peak parameters

Concrete	**Fiber dosage**	σ_{peak} (MPa)	δ_{peak} (μm)	σ_{1000} (MPa)	σ_{2000} (MPa)
	Plain	2.36*	4.9*	—	—
N1 (NSC)	20 kg/m^3	2.19 (± 34%)	5.2 (± 30%)	0.30 (± 80%)	0.28 (± 89%)
	40 kg/m^3	1.81 (± 19%)	5.4 (± 17%)	0.98 (± 58%)	0.95 (± 59%)

* results from two specimens

2.5.4.2. Results of Tests on High Strength Concrete Cores

Figures 2.22-2.24 show the σ-$\bar{\delta}$ response for the HSC specimens. Again, a stable behavior dominates the entire response, which is particularly important in this type of brittle composites. The behavior appears linear up to peak load with a smooth softening after the peak in the case of plain concretes. In the case of SFRCs, the descending branch is followed by post peak hardening up to 500μm, then a plateau up to 1000μm followed by a descending tail. Post-peak stress gains with fiber addition are clear in every case. Again a drop in the σ-$\bar{\delta}$ response is observed around a $\bar{\delta}$ of 30 μm, though it is lower for the case of the higher fiber dosage.

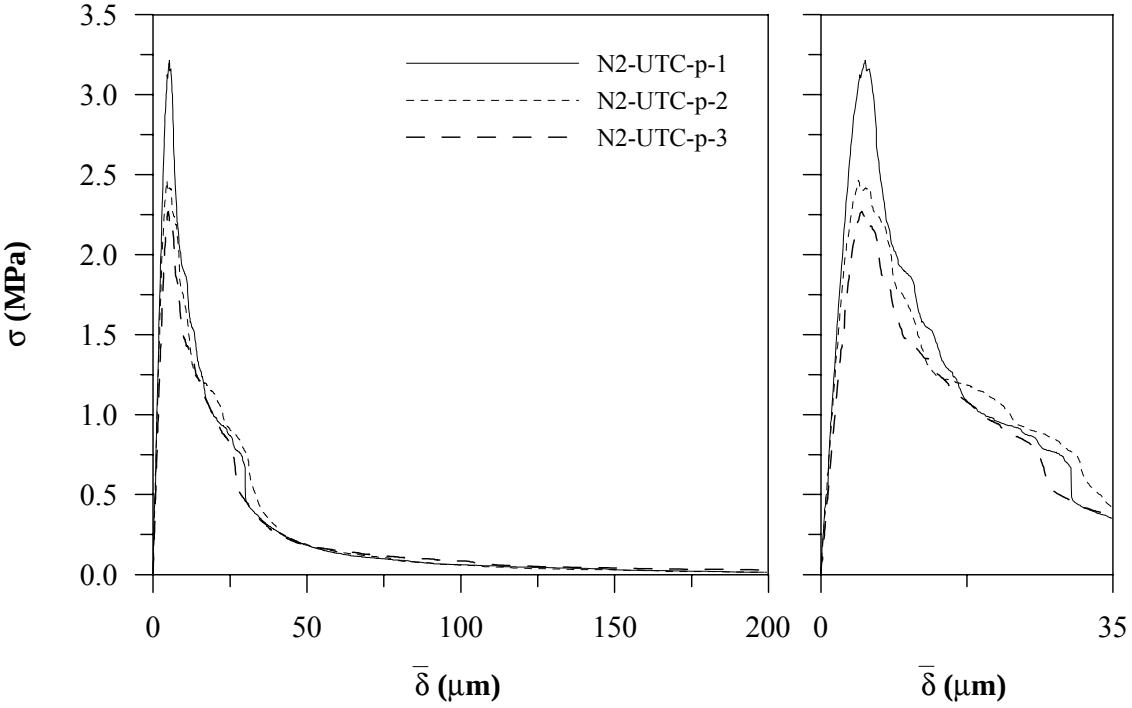

Figure 2.22. σ-$\bar{\delta}$ response for plain HSC cores

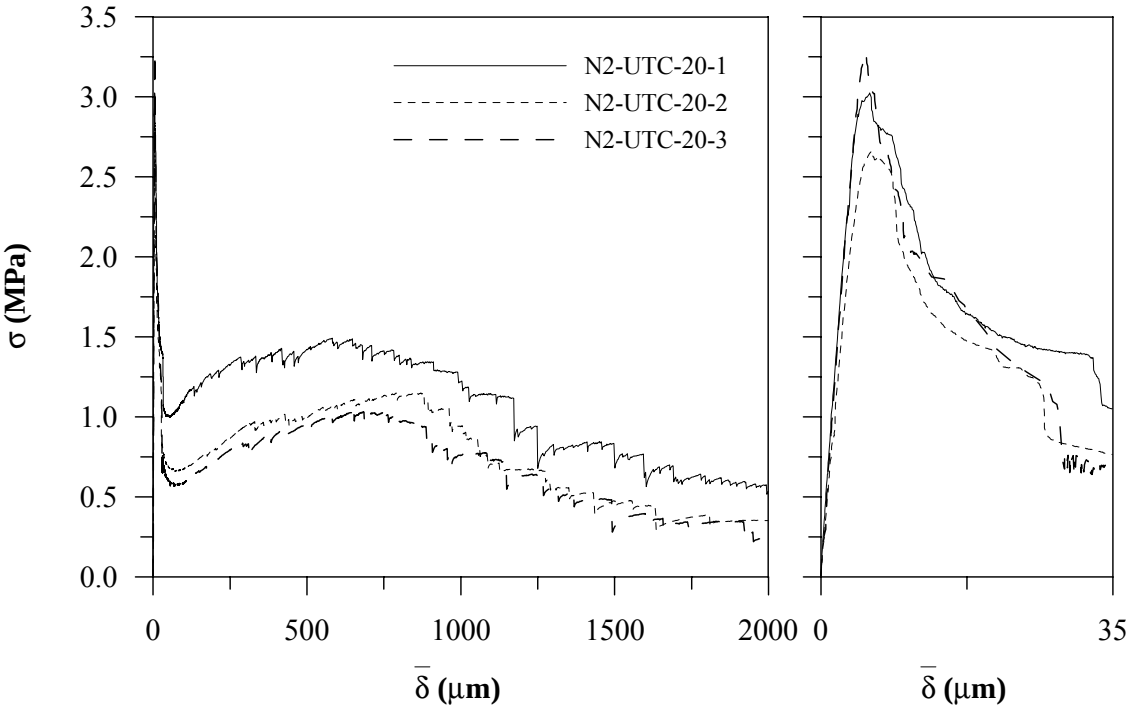

Figure 2.23. σ-$\bar{\delta}$ response for high strength SFRC cores, 20 kg/m^3 of fibers.

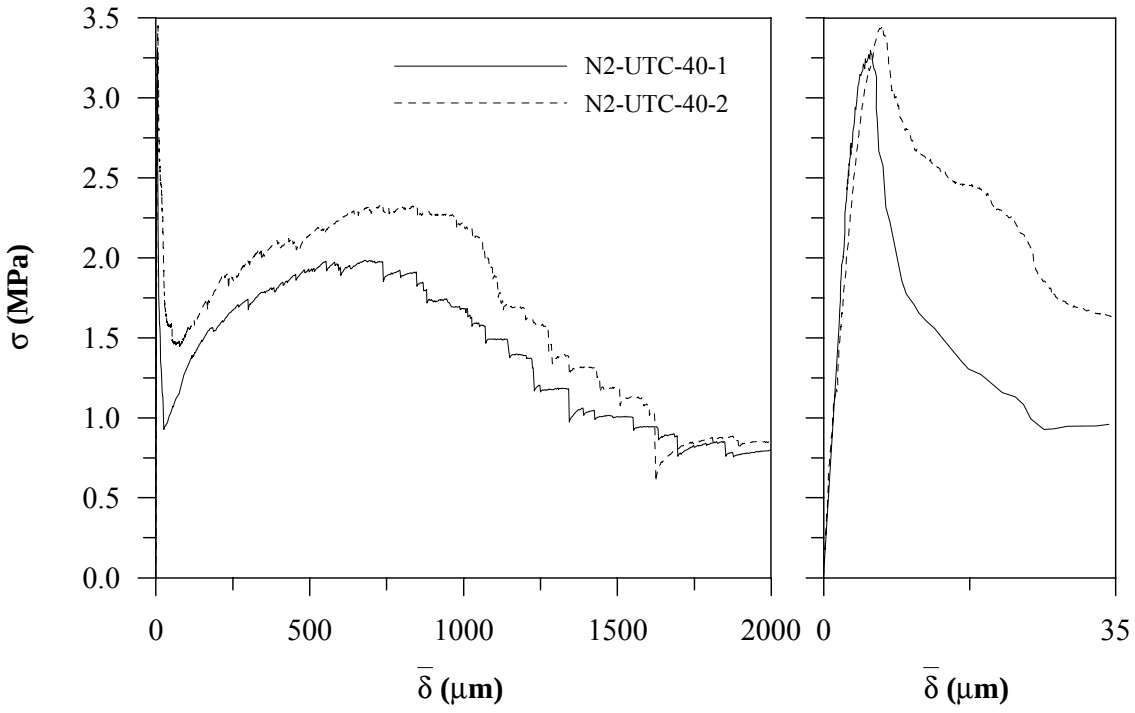

Figure 2.24. σ-$\bar{\delta}$ response for high strength SFRC cores, 40 kg/m^3 of fibers.

Table 2.8 shows the peak and post-peak parameters calculated together with the COV, from which an increase in σ_{peak} with fiber addition can be observed (almost a 28% increase over plain concrete when adding 40 kg/m^3), along with a reduction of the COV. Regarding the post-peak parameters, an important improvement is achieved with fiber dosage, as expected; increasing fiber dosage from 20 to 40 kg/m^3 more than doubles the values of σ_{1000} and σ_{2000}.

Table 2.8. Peak and post-peak parameters

Concrete	**Fiber dosage**	σ_{peak} (MPa)	δ_{peak} (μm)	σ_{1000} (MPa)	σ_{2000} (MPa)
N2 (HSC)	Plain	2.65 (± 19%)	4.9 (± 8.0%)	—	—
	20 kg/m^3	2.99 (± 10%)	5.7 (± 7.0)	0.97 (± 24%)	0.38 (± 38%)
	40 kg/m^3	3.38*	6.0*	1.95*	0.83*

* results from two specimens

2.6. CONCLUSIONS

Considering the tests performed in this chapter, there are several aspects that can be discussed. Firstly, it appears that when a stiff closed-loop testing machine is used, the measurement of individual displacements (δ_i) around the crack mouth is not needed and the direct averaged signal from three transducers is sufficient for control and characterization. Secondly, no practical complications were encountered in the tests of the molded cylinders and cores, with the specimen preparation procedure adopted here. Thirdly, a 10 mm deep notch appears to be insufficient in the case of molded cylinders, where the crack deviated from the notch plane in the normal strength concrete specimens. However, this was not a problem in the tests of cores.

Regarding the σ-$\overline{\delta}$ response, all tests were completely stable and the behavior exhibited an almost linear pre-peak response and a smooth transition to the post-peak regime. The post-peak parameter σ_{2000}, obtained from the σ-$\overline{\delta}$ curve, appears to be sensitive to the fiber content, though the variability is high. It is interesting to note that 52% of the tensile strength can still be supported at a crack opening of 2 mm in the case of the normal strength concrete cores with 40 kg/m^3 of fibers.